Geophysical Journal International

Geophys. J. Int. (2016) **207,** 150–159
Advance Access publication 2016 July 18
GJI Seismology

doi: 10.1093/gji/ggw263

Relative frequencies of seismic main shocks after strong shocks in Italy

Paolo Gasperini,[1,2] Barbara Lolli[2] and Gianfranco Vannucci[2]

[1]*Dipartimento di Fisica e Astronomia, Università di Bologna, Bologna, Italy. E-mail: paolo.gasperini@unibo.it*
[2]*Istituto Nazionale di Geofisica e Vulcanologia, Sezione di Bologna, Bologna, Italy*

Accepted 2016 July 14. Received 2016 July 13; in original form 2016 May 2

SUMMARY

We analysed a catalogue of Italian earthquakes, covering 55 yr of data from 1960 to 2014 with magnitudes homogeneously converted to M_w, to compute the time-dependent relative frequencies with which strong seismic shocks ($4.0 \leq M_w < 5.0$), widely felt by the population, have been followed by main shocks ($M_w \geq 5.0$) that threatened the health and the properties of the persons living in the epicentral area. Assuming the stationarity of the seismic release properties, such frequencies are estimates of the probabilities of potentially destructive shocks after the occurrence of future strong shocks. We compared them with the time-independent relative frequencies of random occurrence in terms of the frequency gain that is the ratio between the time-dependent and time-independent relative frequencies. The time-dependent relative frequencies vary from less than 1 per cent to about 20 per cent, depending on the magnitudes of the shocks and the time windows considered (ranging from minutes to years). They remain almost constant for a few hours after the strong shock and then decrease with time logarithmically. Strong earthquakes (with $M_w \geq 6.0$) mainly occurred within two or three months of the strong shock. The frequency gains vary from about 10 000 for very short time intervals to less than 10 for a time interval of 2 yr. Only about 1/3 of main shocks were preceded by at least a strong shock in the previous day and about 1/2 in the previous month.

Key words: Earthquake interaction, forecasting, and prediction; Statistical seismology.

INTRODUCTION

It is well known that seismic shocks tend to cluster in time and space (Mulargia & Geller 2003; Kagan 2014). In the days, weeks and months after the main shock the rate of smaller shocks (called aftershocks) in the same area (usually within a radius of some tens of km from the main shock for a moderate magnitude earthquake) is definitely higher than before the main shock. The aftershock rate typically decays with time following an empirical power law first observed by Omori (1894), but also other models of aftershock decay have been proposed in the literature (e.g. Kisslinger 1993; Narteau *et al*. 2003; Lolli *et al*. 2011).

Even before the main shock, rates of shocks higher than the long-term average are sometimes observed. Seismic clustering was also observed at longer times (of the order of years and tens of years) and longer distances (of the order of hundreds or thousands of km; e.g. Kagan & Jackson 1991; Mulargia & Geller 2003; Marzocchi & Lombardi 2008, 2009a; Parsons *et al*. 2015).

The physical reasons of seismic clustering are not yet fully understood but in general they are related to stress state variations within the solid earth (Dieterich 1994). Each shock modifies this state and may then trigger the occurrence of other shocks. This approach is the basis of the Epidemic Type Aftershock Sequence model (Ogata 1988) where each shock that occurred is assumed to contribute to the triggering of the following shocks, depending on its size (magnitude) and on the closeness in time and space to the triggered shocks (Console & Murru 2001; Console *et al*. 2003; Marzocchi & Lombardi 2009b).

Various computational strategies based on preceding seismicity have been proved to forecast main shocks better than the purely random (Poissonian) occurrence assumption (Jordan *et al*. 2011). It is generally thought that the occurrence of strong shocks in a previously quiet area increases the probability of occurrence of a destructive shock by some orders of magnitude but this evidence is difficult to use for practical forecasts because the probabilities of occurrence usually remain of the order of few percent at most (Jordan *et al*. 2011, 2014). Another difficulty is related to the delay between the issuing of the forecast and its public diffusion to the population by the media. Hence, the shortest-term forecasts are usually issued on a daily basis (e.g. Marzocchi & Lombardi 2009b). This leaves open the problem of what to do in the minutes or hours just after the occurrence of a strong shock before a warning message is issued by civil protection services.

The occurrence of a strong non-destructive seismic shock frightens the population, and they usually escape outdoors even during the shock (although this is not recommended by seismic engineers) and wait for a certain amount of time before returning indoors. Although this practice is widespread, a precise policy on what to do in these situations has not been established yet, particularly concerning the time to stay outside in order to reduce the risk of being involved in building collapse owing to a successive destructive shock.

If the persons feeling the shock are located close to the epicentre, the magnitude of the strong shock might be roughly estimated by the observed macroseismic effects. According to common relationships between magnitude and epicentral intensity (I_0) estimated for Italy (e.g. Gasperini 2004), a shock with $M_w = 4.0$ about corresponds to I_0 = IV–V, which means that the shock was felt at the epicentre by most and no damage to buildings occurred, while a shock with $M_w = 4.5$ about corresponds to I_0 = V–VI, which means that the shock was felt by all with fear and only slight damage to buildings may have occurred (Sieberg 1931; Grünthal 1998).

Accordingly, a shock with $M_w = 5.0$ corresponds on average to I_0 = VII (slight to moderate damage to buildings depending on their robustness), a shock with $M_w = 5.5$ corresponds to I_0 = VIII (heavy damage with few collapses) and a shock with $M_w = 6.0$ corresponds to I_0 = IX (very heavy damage with widespread collapses of weak buildings). Casualties and injuries are usually possible but infrequent for $M_w = 5.0$, likely for $M_w = 5.5$ and almost certain for $M_w = 6.0$.

We analyse the Italian seismicity from 1960 to 2014 as reported by a seismic catalogue homogenized in terms of M_w (Gasperini *et al*. 2013; Lolli *et al*., in preparation) to estimate the relative frequencies with which strong shocks were actually followed by destructive shocks in the same area (within a radius of some tens of km from the epicentre of the strong shock) and within various successive time intervals. Assuming the stationarity of seismic generation properties, such frequencies correspond to approximate estimates of the probabilities (e.g. Kalbfleish 1985) of future potentially destructive shocks. These probabilities do not depend on the assumption of any seismic occurrence model but only on the hypothesis of the stationarity of seismic release properties at the Italian scale. Similar analyses with different procedures have been proposed in the past by Jones (1984, 1985, 1995) and Agnew & Jones (1991) in Southern California, Savage & De Polo (1993) in Great Basin, Nevada, and by Grandori *et al*. (1988) and Di Luccio *et al*. (1993, 1997, 1999) in Italy.

We define as 'strong' a shock that is widely felt by the population in the epicentral area but usually without significant damage to the buildings. In the following we will consider them within two different magnitude ranges: (1) $4.0 \le M_w < 4.5$ and (2) $4.5 \le M_w < 5.0$. According to the correspondences with epicentral intensity mentioned above, the former range corresponds to a shock that usually does not produce any damage to buildings while the latter to a shock that may sometimes produce some moderate damage but very likely does not threaten the lives of the people staying inside or close to the buildings. We must note that, based on the Gutenberg & Richter (1944) law (with $b \approx 1$), about 2/3 (64 per cent) of the shocks within 0.5 units wide intervals (4.0–4.5 and 4.5–5.0) have a magnitude closer to the lower bounds (4.0 and 4.5, respectively) than to the upper bounds (4.5 and 5.0).

We define the target potentially destructive *main shocks* as those exceeding thresholds $M_w \ge 5.0$, $M_w \ge 5.5$ and $M_w \ge 6.0$. Larger thresholds cannot be investigated because only one shock with $M_w \ge 6.5$ (1980, $M_w = 6.8$, Irpinia earthquake) did occur during the 55 yr time interval covered by our seismic catalogue. We consider as well spatial ranges Δr from the epicentre of the strong shock of 20, 30 and 50 km.

HOMOGENIZED CATALOGUE OF ITALIAN INSTRUMENTAL SEISMICITY FROM 1960 TO 2014

For the time interval from 1981 to 2014, we go with Gasperini *et al*. (2013) who used general orthogonal regressions (GORs; Fuller 1987; Stromeyer *et al*. 2004; Castellaro *et al*. 2006) to derive conversion equations from various types of local magnitude definitions to moment magnitude M_w. We also include in the catalogue real M_w magnitudes from an integrated data set compiled by Gasperini *et al*. (2012) based on Moment Tensor solutions available for Italy from various sources: the Global Centroid Moment Tensor catalogue (Dziewoński *et al*. 1981; Ekström *et al*. 2012), the National Earthquake Information Center (NEIC) Moment Tensor catalogue (Sipkin 1982, 1994), the European–Mediterranean Regional Centroid Moment Tensor catalogue (Pondrelli *et al*. 2006, 2011), the Eidgenössische Technische Hochschule Zürich (ETHZ) Moment Tensor catalogue (Braunmiller *et al*. 2002) and the Time Domain Moment Tensor catalogue of the Istituto Nazionale di Geofisica e Vulcanologia (INGV, formerly known as ING; Scognamiglio *et al*. 2009). The preferred sources of the hypocentral parameters we used here, from 1981 to 1996, the *Catalogo Strumentale dei Terremoti Italiani* (CSTI) Version 1.1 (CSTI Working Group 2005); from 1997 to 2002, the *Catalogo della Sismicità Italiana* (CSI) Version 1.1 (Castello *et al*. 2007); from 2003 to 15 April 2005, the *Bollettino Sismico Italiano* (BSI) of the INGV; and from 16 April 2005 to 2014 the ISIDe Bulletin of INGV (Amato *et al*. 2006). The resulting data set contains 245 405 events, 218 526 of which have an M_w magnitude estimate (real or proxy) with a related error. Such data set has been found by Gasperini *et al*. (2013) to be reasonably complete from 1981 to 2010 for $M_w \ge 3$.

For the time interval from 1960 to 1980, we use a preliminary version of a data set mainly based on the *Catalogo del Progetto Finalizzato Geodinamica* (PFG; Postpischl 1985) and integrated with locations from the bulletins of the ING and of the International Seismological Center (ISC). We also integrate magnitudes with data of two couples of Wood–Anderson seismometers (Anderson & Wood 1925), operating in Italy in the 1970s and 1980s at the Trieste (TRI) and Roma Monte Porzio (RMP) stations, which we derived from a careful scrutiny of paper bulletins of the Osservatorio Geofisico Sperimentale (OGS, now known as INOGS) and ING by Lolli *et al*. (in preparation). Magnitudes provided by the PFG catalogue and other data sources are calibrated with respect to M_w by GORs similar to those used by Gasperini *et al*. (2013). The final data set contains 8754 events, 5455 of which have an M_w magnitude estimate with a related error.

The analysis of the frequency-magnitude distribution (Gutenberg & Richter 1944) of this portion of the catalogue (Fig. 1) indicates an acceptable completeness for $M_w \ge 4.0$. Then we can take as complete the entire catalogue from 1960 to 2014 for $M_w \ge 4.0$. Such completeness threshold might eventually increase in the periods immediately following main shocks owing to the difficulty of locating aftershocks due to the superposition of the waveform recorded at seismic stations. However, our analyses are scarcely influenced by this incompleteness as we focus on the periods preceding main shocks.

As intermediate and deep earthquakes are known to have different occurrence properties with respect to shallower ones, we exclude from our analysis all shocks with depth $h > 50$ km. In summary, the data set with $M_w \ge 4.0$ we use for our analyses includes in all 1613 shocks from 1960 to 2014 (Table 1).

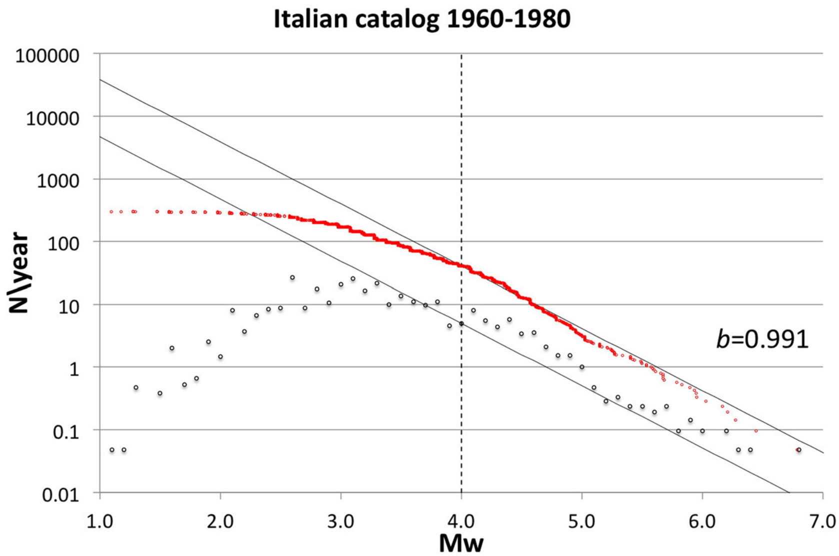

Figure 1. Cumulative (red dots) and non-cumulative (black circles) frequency–magnitude distribution (Gutenberg & Richter 1944) for the integrated and homogenized catalogue of Italian earthquakes from 1960 to 1980.

Table 1. Number of shocks in the data set as a function of M_w.

Magnitude class	N
$M_w \geq 4.0$	1613
$M_w \geq 4.5$	476
$M_w \geq 5.0$	121
$M_w \geq 5.5$	35
$M_w \geq 6.0$	7
$M_w \geq 6.5$	1

For prospective use of our analyses, ML magnitudes provided in near real-time by the ISIDe bulletin of INGV can be converted to M_w, according to Gasperini *et al*. (2013), by the equation

$$M_w = 1.066\,\mathrm{ML} - 0.164 \quad (1)$$

with the related error given by the equation

$$\sigma_{M_w} = \sqrt{\mathrm{ML}^2 \cdot 0.031^2 + 0.127^2 - 2\mathrm{ML} \cdot 0.0038 + 1.066^2 \cdot 0.18^2}. \quad (2)$$

This means that the error slightly increases from about 0.18 m.u. of ISIDe ML to about 0.20 m.u. of the M_w proxy.

RESULTS

We compute the time-dependent relative frequency f_d with which *strong shocks* were followed by *main shocks* as

$$f_d = \frac{n}{N} \quad (3)$$

where n is the number of *strong shocks* followed by at least a *main shock* within a time interval Δt and within a distance range Δr, and N is the total number of *strong shocks* in the catalogue. Assuming the stationarity of earthquake occurrence properties, this is an approximate estimate of the probability that a future *strong shock* is followed by a *main shock* within given time intervals.

We also compute for comparison the time-independent relative frequency f_i with which *strong shocks* occurred within a spatial range Δr from any *main shock* in the catalogue and within any time window Δt as

$$f_i = \frac{k}{N} \frac{\Delta t}{\Delta t_{\mathrm{tot}}}, \quad (4)$$

where k is the number of *strong shocks* within a range Δr from any *main shock* which occurred over the entire time window Δt_{tot} covered by the catalogue (55 yr).

We exclude from such counts *strong shocks* which occurred within a time window Δt at the end of the catalogue as they might have been followed by *main shocks* occurring after the ending date (2014 December 31).

The ratio

$$g = \frac{f_d}{f_i} \quad (5)$$

corresponds to the relative frequency gain after the occurrence of a *strong shock* within the given time window.

We also compute the relative frequency f_m with which *main shocks* were preceded by *strong shocks* as

$$f_m = \frac{m}{M}, \quad (6)$$

where m is the number of *main shocks* preceded by at least a *strong shock* within a time interval Δt and a distance range Δr, and M is the total number of *main shocks* in the catalogue. In this case we exclude from the counts *main shocks* that eventually occurred within a time window Δt at the beginning of the catalogue as they might have been preceded by *strong shocks* that occurred before the starting date (1960 January 1).

In Fig. 2, top panel, we display the relative frequencies f_d of *strong shocks* with $4.0 \leq M_w < 4.5$ followed by *main shocks*. For *main shocks* with $M_w \geq 6.0$ (red), the frequencies are lower than 1 per cent for any time window Δt after the *strong shock*. Note that these about correspond to the probability of the $M_w = 6.3$ L'Aquila earthquake of 2009 April 6 after a strong shock with $M_w = 4.4$ occurred about a week before on 2009 March 30.

For *main shocks* with $M_w \geq 5.0$ (blue) and $M_w \geq 5.5$ (green), relative frequencies show a logarithmically increasing trend with the duration Δt of the time window that becomes slightly steeper, starting from a Δt of one day. The frequencies within one day are

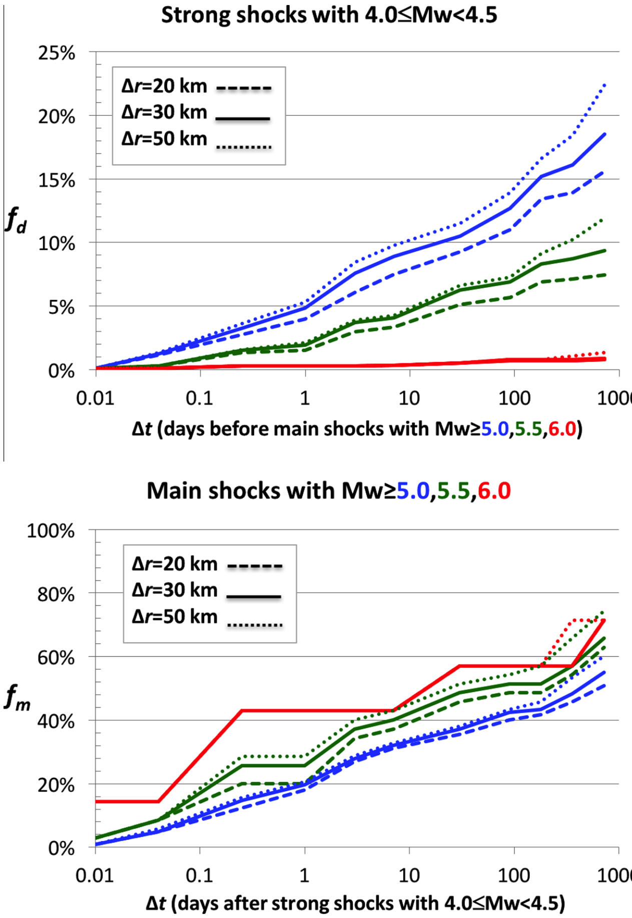

Figure 2. Top: relative frequencies of *strong shocks* with $4.0 \leq M_w < 4.5$ that have been followed, within a distance $\Delta r = 20$ (dashed), 30 (solid) and 50 (dotted) km, by *main shocks* with $M_w \geq 5.0$ (blue), $M_w \geq 5.5$ (green) and $M_w \geq 6.0$ (red) as a function of the time window Δt before the *main shock*. Bottom: relative frequencies of *main shocks* with $M_w \geq 5.0$ (blue), $M_w \geq 5.5$ (green) and $M_w \geq 6.0$ (red) that have been preceded, within a distance $\Delta r = 20$ (dashed), 30 (solid) and 50 (dotted) km, by a *strong shock* with $4.0 \leq M_w < 4.5$, as a function of the time window Δt after the *strong shock*.

about 5 per cent for a *main shock* with $M_w \geq 5.0$ and about 2 per cent for $M_w \geq 5.5$; for the longest time window of 2 yr they range from 7 per cent to 12 per cent and from 15 per cent to 22 per cent, respectively. The differences between the various spatial ranges we tested, 20 (dashed), 30 (solid) and 50 (dotted) km, are very small for $M_w \geq 6.0$ and relatively small at short time windows for the other two magnitude thresholds. The maximum difference, for the longest time window of 2 yr, is of the order of 3 per cent.

In Fig. 2, bottom panel, the relative frequencies of *main shocks* preceded by *strong shocks* with $4.0 \leq M_w < 4.5$ within given time and space windows are reported. They show a relatively low variability with the spatial range Δr and with the magnitude of the *main shock*. Only 20 per cent of *main shocks* with $M_w \geq 5.0$ and 25 per cent with $M_w \geq 5.5$ have been actually preceded by *strong shocks* with $4.0 \leq M_w < 4.5$ on the previous day. For *main shocks* with $M_w \geq 6.0$ the relative frequency of the previous day is higher but still lower than 50 per cent (about 43 per cent). Considering a time window of one month, relative frequencies range from 37 per cent for $M_w \geq 5.0$ to 57 per cent for $M_w \geq 6.0$. For the longest time window of 2 yr, the frequencies range between 50 per cent and 70 per cent. The differences between various spatial ranges are generally small and become of the order of 5 per cent only for the longest time windows.

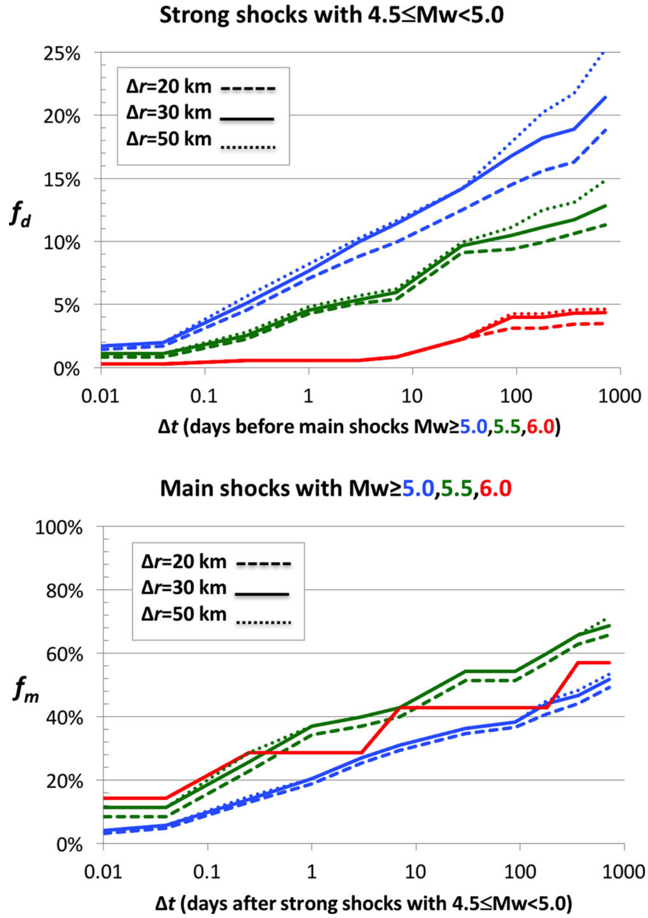

Figure 3. Same as Fig. 2 for *strong shocks* with $4.5 \leq M_w < 5.0$.

Fig. 3 shows the results of the same computations for *strong shocks* with $4.5 \leq M_w < 5.0$. With respect to the previous case, we can note a general increase in the relative frequency of *strong shocks* followed by *main shocks* (top) and a decrease in the frequency of *main shocks* preceded by *strong shock* (bottom).

For a Δt of one day, the relative frequencies of *strong shocks* with $4.0 \leq M_w < 4.5$ followed by *main shocks* are about 7 per cent for $M_w \geq 5.0$, 4 per cent for $M_w \geq 5.5$ and 0.5 per cent $M_w \geq 6.0$. For the latter magnitude threshold we can note a clear increase in the frequency from about 1 per cent to 4 per cent for Δt going from 7 d to 3 months. The frequencies for a time window of 1 month are of the order of 14 per cent for $M_w \geq 5.0$, 9 per cent for $M_w \geq 5.5$ and 2 per cent for $M_w \geq 6.0$. For the longest windows of 2 yr, they are of the order of 22 per cent, 13 per cent and 4 per cent, respectively. Relative frequencies for other time windows Δt for the spatial range $\Delta r = 30$ km are reported in Table 2.

A direct comparison between the two foreshock definitions is shown in Fig. 4 where the relative frequency gains (ratios between the time-dependent and time-independent relative frequencies) are displayed. For *strong shocks* with $4.0 \leq M_w < 4.5$ (top), the gains range from about 10 000 for the shortest Δt (of the order of minutes to hours) to less than 10 for the longest Δt (1 or 2 yr). In particular, for *main shocks* with $M_w \geq 6.0$, the relative frequency gain for the longest interval becomes close to 1, thus indicating a time-dependent relative frequency almost reaching the time-independent one. We note the peculiar case of the curves for $M_w \geq 5.0$ (blue)

Table 2. Relative frequencies f_d of strong shocks followed by main shocks within $\Delta r = 30$ km and various Δt.

Strong shock	$4.0 \le M_w < 4.5$			$4.5 \le M_w < 5.0$		
Main shock	$M_w \ge 5.0$	$M_w \ge 5.5$	$M_w \ge 6.0$	$M_w \ge 5.0$	$M_w \ge 5.5$	$M_w \ge 6.0$
$\Delta t = 15$ min	0.1%	0.1%	0.1%	1.7%	1.1%	0.3%
$\Delta t = 1$ hr	1.2%	0.3%	0.1%	2.0%	1.1%	0.3%
$\Delta t = 6$ hr	3.3%	1.5%	0.3%	5.1%	2.5%	0.6%
$\Delta t = 1$ d	4.8%	1.9%	0.3%	7.6%	4.5%	0.6%
$\Delta t = 3$ d	7.6%	3.7%	0.3%	9.9%	5.4%	0.6%
$\Delta t = 7$ d	8.9%	4.1%	0.4%	11.4%	6.0%	0.9%
$\Delta t = 1$ month	10.5%	6.3%	0.5%	14.2%	9.7%	2.3%
$\Delta t = 3$ months	12.7%	6.9%	0.8%	16.8%	10.5%	4.0%
$\Delta t = 6$ months	15.2%	8.3%	0.8%	18.2%	11.1%	4.0%
$\Delta t = 1$ yr	16.1%	8.7%	0.8%	18.9%	11.7%	4.3%
$\Delta t = 2$ yr	18.5%	9.4%	0.9%	21.4%	12.8%	4.4%

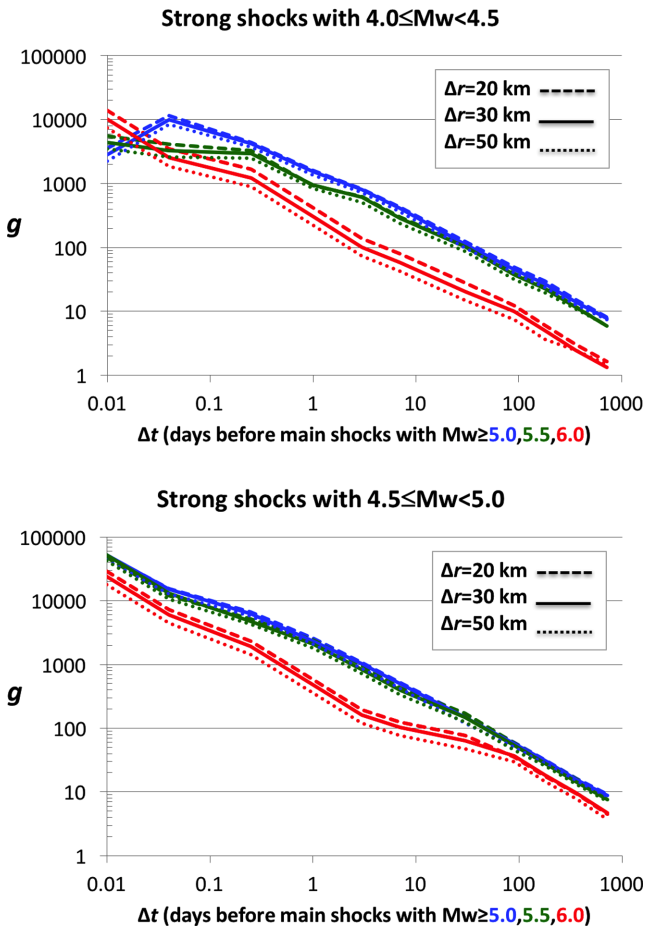

Figure 4. Frequency gain for the occurrence of *main shocks* within given space (Δr) and time (Δt) windows after the occurrence of *strong shocks* with $4.0 \le M_w < 4.5$ (top) or $4.5 \le M_w < 5.0$ (bottom).

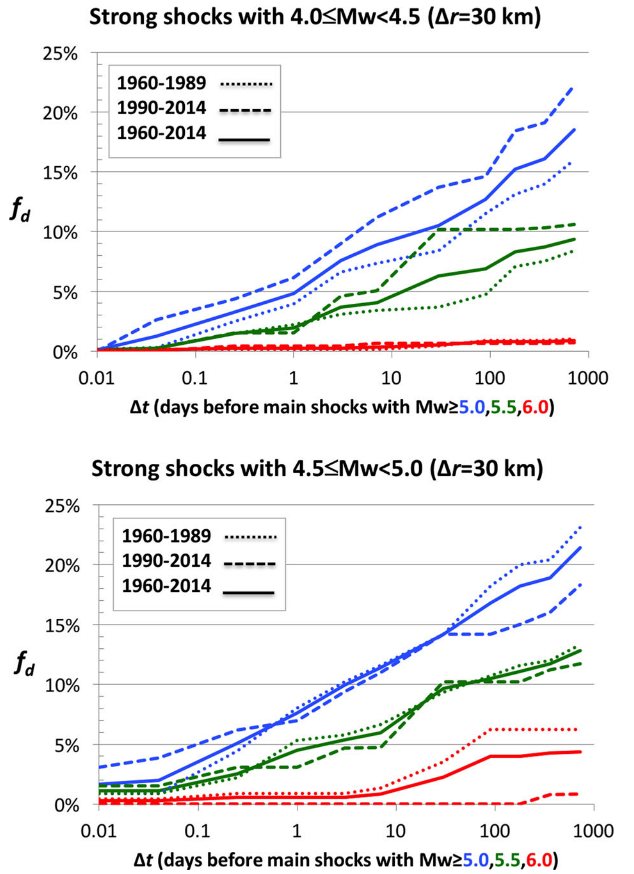

Figure 5. Relative frequencies of *strong shocks* with $4.0 \le M_w < 4.5$ (top) and $4.5 \le M_w < 5.0$ (bottom) that have been followed, within a distance $\Delta r = 30$ km, by *main shocks* with $M_w \ge 5.0$ (blue), $M_w \ge 5.5$ (green) and $M_w \ge 6.0$ (red) as a function of the time window Δt before the *main shock*, in different time intervals: 1960–1989 (dotted), 1990–2014 (dashed) and 1960–2014 (solid).

that are not monotonically decreasing at short Δt's. This could suggest the existence of some sort of incompleteness for this class of *strong shocks* as, particularly in the earliest times of the catalogue, a *strong shock* of this class might have been masked by an almost simultaneous shock with a larger magnitude.

For *strong shocks* with $4.5 \le M_w < 5.0$ (bottom), the frequency gains are generally larger and less differentiated than for the magnitude range $4.0 \le M_w < 4.5$ and, for all the three *main shock* thresholds, they are monotonically decreasing even at short Δt.

As relative frequencies, for both definitions of *strong shock*, show a scarce dependence on the spatial range Δr, in the following we will only consider the intermediate range $\Delta r = 30$ km.

In Fig. 5, we test the stability with time of relative frequencies of *strong shocks* followed by *main shocks* by comparing the results obtained over the entire time interval from 1960 to 2014 covered by our catalogue (solid lines) with those obtained within two disjointed time intervals from 1960 to 1989 (dotted) and from 1990 to 2014 (dashed). The choice of the dividing epoch was suggested by the fact that since 1990 the quality of the Italian National Seismic

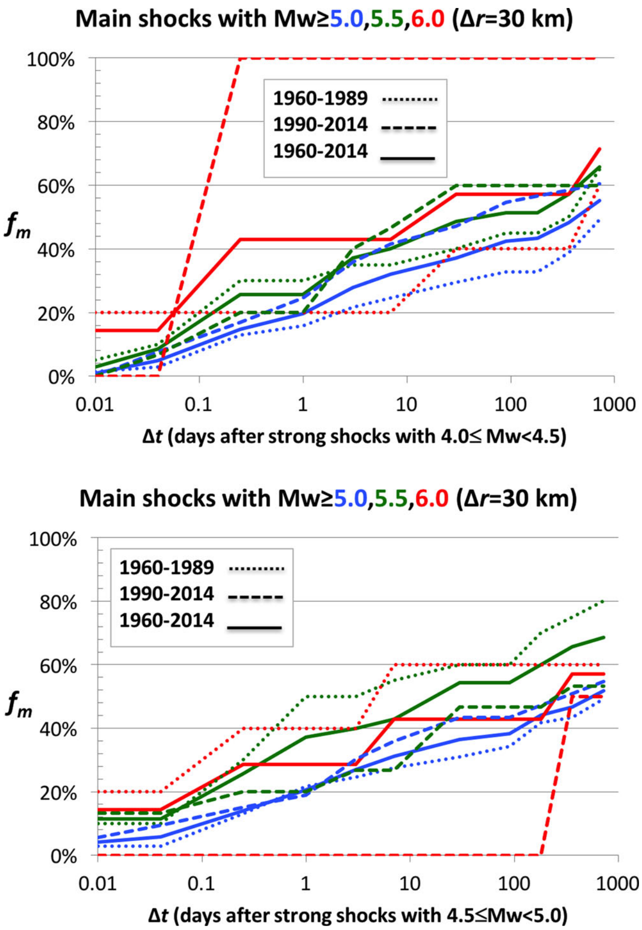

Figure 6. Relative frequencies of *main shocks* with $M_w \geq 5.0$ (blue), $M_w \geq 5.5$ (green) and $M_w \geq 6.0$ (red) that have been preceded, within a distance $\Delta r = 30$ km, by a *strong shock* with $4.0 \leq M_w < 4.5$ (top) and $4.5 \leq M_w < 5.0$ (bottom), as a function of the time window Δt after the *strong shock*, in different time intervals: 1960–1989 (dotted), 1990–2014 (dashed) and 1960–2014 (solid).

Network of INGV improved significantly as testified to, for example, by the decrease of the completeness threshold from about $M_w = 3.0$ to $M_w = 2.5$ (Gasperini *et al.* 2013). Relative frequencies for *strong shocks* with $4.0 \leq M_w < 4.5$ are slightly higher in the most recent period (1990–2014, dashed) with respect to the preceding one (1960–1989, dotted), but for both periods they are substantially consistent with those computed for the entire time interval (1960–2014, solid). For *strong shocks* with $4.5 \leq M_w < 5.0$, we observe a substantial stability for *main shocks* with $M_w \geq 5.0$ and $M_w \geq 5.5$, whereas for *main shocks* with $M_w \geq 6.0$ we can note definitely higher frequencies at long Δt for the antecedent time interval with respect to the subsequent one. This inconsistency might be due to the chance, owing to the very low number (2) of *main shocks* with $M_w \geq 6.0$ in the most recent time interval from 1990 to 2014.

The same stability analysis is shown in Fig. 6 for relative frequencies of *main shocks* preceded by *strong shocks*. Relative frequencies are generally higher in the most recent period for *strong shocks* with $4.0 \leq M_w < 4.5$ and in the antecedent one for *strong shocks* with $4.5 \leq M_w < 5.0$. Note the peculiar behaviour, for strong shocks with $4.0 \leq M_w < 4.5$ (Fig. 6 top) in the most recent period, of the frequencies for the largest magnitude class of *main shocks* ($M_w \geq 6.0$, red dashed) that reaches 100 per cent starting from $\Delta t = 6$ hr as the two *main shocks* with $M_w \geq 6.0$ occurred in Italy since 1990 (on 2009 April 6, $M_w = 6.3$ in L'Aquila and 2012 May 20, $M_w = 6.1$ in Emilia) have been preceded a few hours before by *strong shocks* with $M_w = 4.4$ and $M_w = 4.3$, respectively. We can see as well that for *strong shocks* with $4.5 \leq M_w < 5.0$ (Fig. 6 bottom) in the most recent period, relative frequencies for *main shocks* with $M_w \geq 6.0$ (red dashed) are zero up to about $\Delta t = 1$ yr when they become 50 per cent, as only one of the two *main shocks* (Emilia) has been preceded by a *strong shock* (with $M_w = 4.8$) about 8 months before (on 2011 July 17).

The computations shown above only represent 'static' pictures taken just at the time of occurrence of the *strong shock*. However, as the time flows after the *strong shock*, relative frequencies vary with time and, if a *main shock* actually does not occur, progressively decrease towards the long time average (time-independent). In the following, we show the behaviour of relative frequencies of *strong shocks* followed by *main shocks* computed over time windows Δt that start, rather than at the time of the *strong shock*, at successive times after it, under the condition that no *main shocks* have occurred in the meantime.

For varying t_{start}, we compute

$$f_d\left(t_{\mathrm{start}}\right) = \frac{n\left(t_{\mathrm{start}}\right)}{N\left(t_{\mathrm{start}}\right)}, \tag{7}$$

where $n(t_{\mathrm{start}})$ is the number of *strong shocks* followed by at least a *main shock* within a spatial range Δr and within a time interval of length Δt starting at t_{start}, and $N\left(t_{\mathrm{start}}\right)$ is the number of all *strong shocks* considered in the analysis for each t_{start}. The variation of t_{start} terminates if a *main shock* occurs within the time window.

Fig. 7 shows the result of such computations for *strong shocks* with $4.0 \leq M_w < 4.5$. Each curve represents the time evolution of the relative frequency for a given time window Δt as a function of the start time t_{start} of the window.

We can note that for *main shocks* with $M_w \geq 5.0$ (top) and $M_w \geq 5.5$ (middle), the relative frequencies remain rather constant and close to the initial values ($t_{\mathrm{start}} = 0$) for about 40 and 80 min, respectively, after the main shock then they start to decrease logarithmically at an almost constant rate of about 0.7–1.0 per cent for each doubling of t_{start}. For *main shocks* with $M_w \geq 6.0$ (bottom), the behaviour is rather irregular owing to the scarce number of data but we can note a clear decrease of 0.1 per cent for most curves a few minutes after the *strong shock* and a further decrease of about 0.2 per cent after about 5 hr. For almost all Δt's, relative frequencies decrease below 0.1 per cent two or three months after the strong shock.

In Fig. 8, showing the same computations for *strong shocks* with $4.5 \leq M_w < 5.0$, we can see similar behaviours for *main shocks* with $M_w \geq 5.0$ (top) and $M_w \geq 5.5$ (middle), whereas, for *main shocks* with $M_w \geq 6.0$ (bottom), relative frequencies remain in most cases rather constant for some days after the *strong shocks* when they start to decrease quickly. Even in this case relative frequencies go below 0.1–0.2 per cent two to three months after the strong shock.

CONCLUSIONS

We analysed a homogenized catalogue of Italian seismicity from 1960 to 2014 to compute the relative frequencies with which strong shocks widely felt by the population were followed in the same area by main shocks threatening the goods and the lives of the inhabitants. Under the assumption of stationarity of the seismic release properties, such frequencies are approximate estimates of the probabilities of occurrence of main shocks after the occurrence of future strong shocks. The accuracy of such approximation was evaluated

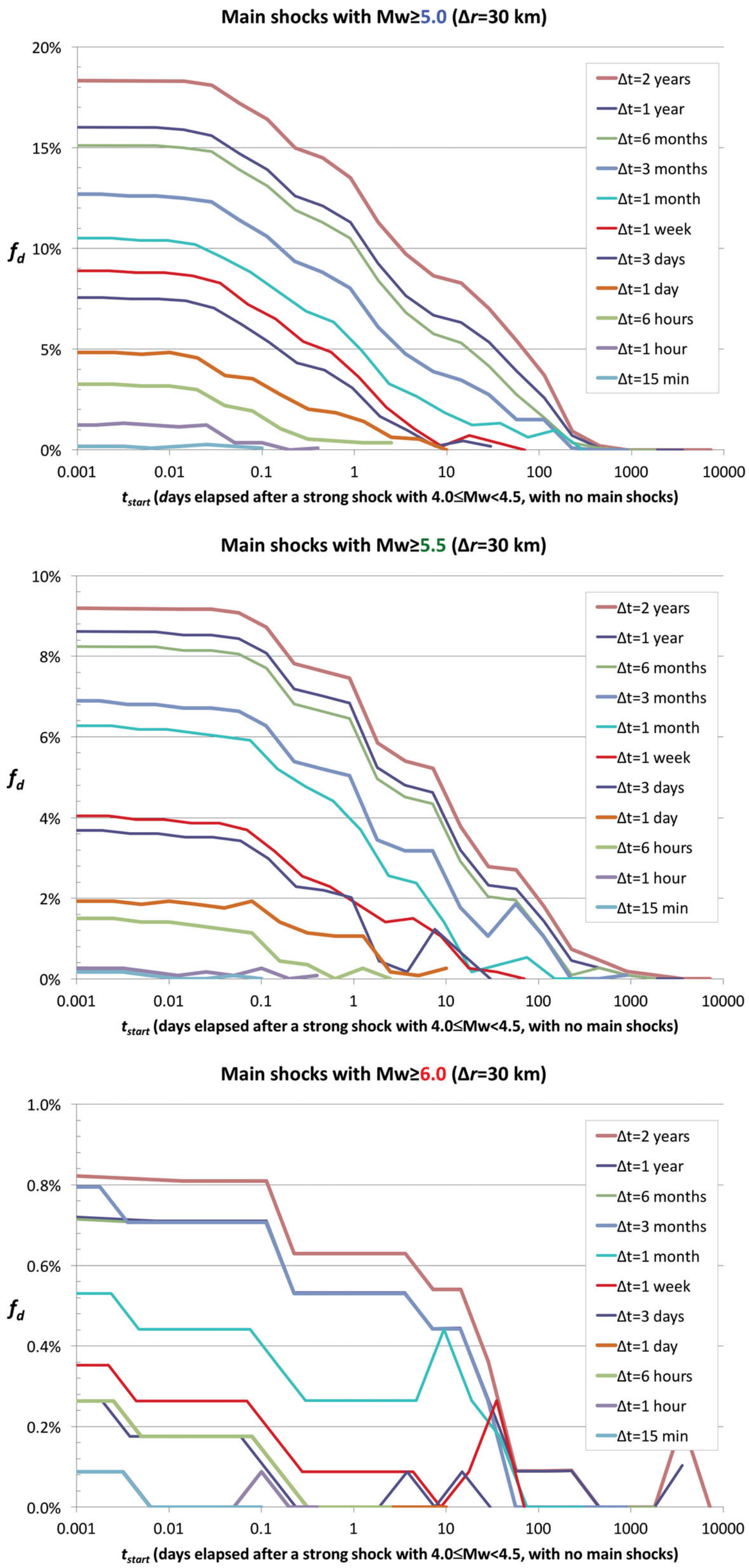

Figure 7. Evolution of relative frequencies of *strong shocks* with $4.0 \le M_w < 4.5$ that have been followed by *main shocks* with $M_w \ge 5.0$ (top), $M_w \ge 5.5$ (middle) and $M_w \ge 6.0$ (bottom), within a distance $\Delta r = 30$ km and within different time windows Δt starting at times t_{start} after the *strong shock*, on condition that before t_{start} no *main shocks* have occurred.

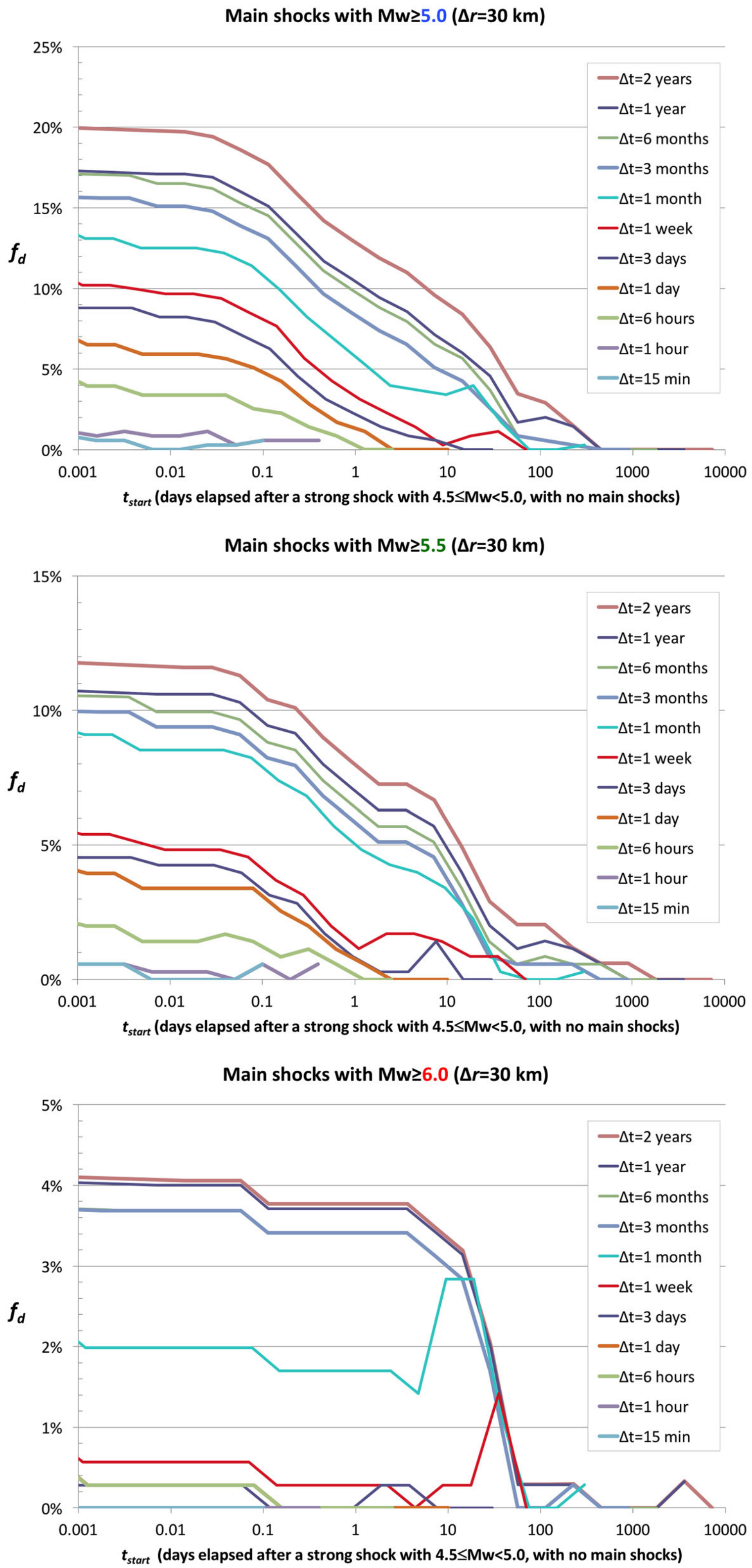

Figure 8. Same as Fig. 7 for *strong shocks* with $4.5 \leq M_w < 5.0$.

by the separate analysis over two disjointed time intervals (before and after the beginning of 1990) showing a substantial stability of relative frequencies excepting the largest class of main shocks considered ($M_w \geq 6.0$). The latter instability can be justified by the low number of main shocks of such magnitude class which occurred in Italy since 1990 (only 2).

Our analysis indicates that the occurrence of a *strong shock* greatly increases the probability of occurrence of a potentially destructive *main shock* with respect to quiet periods by a factor (probability gain) of about 10 000 or more that. Then, as time goes by, it decreases logarithmically down to less than a factor of 10 for time windows of months or years.

The probability of a very large *main shock* ($M_w \geq 6.0$) is generally lower than 1 per cent except from about one month after a *strong shock* with $4.5 \leq M_w < 5.0$ when it becomes of the order of 4 per cent, but it decreases well below 1 per cent about two or three months after the *strong shock* if the *main shock* did not actually occur in the meantime.

Just after the occurrence of a strong shock, the probability of main shocks with $M_w \geq 5.0$ and $M_w \geq 5.5$ within one day range from 5 per cent to 2 per cent and within one month from 14 per cent to 6 per cent. They remain quite stable for about one hour after the *strong shock* and then start to decrease logarithmically at a rate of about 1 per cent for each doubling of the time elapsed from the strong shock.

Only about 30 per cent of main shocks have been preceded by strong shocks within one day, about 50 per cent within one month and about 60 per cent within 1 yr. This means that about half of all main shocks were not preceded by any precursory shock within reasonable time windows.

REFERENCES

Agnew, D.C. & Jones, L.M., 1991. Prediction probabilities from foreshocks, *J. geophys. Res.*, **96**, 11 959–11 971.

Amato, A., Badiali, L., Cattaneo, M., Delladio, A., Doumaz, F. & Mele, F., 2006. The real-time earthquake monitoring system in Italy, *Geosciences (BGRM)*, **4**, 70–75.

Anderson, J.A. & Wood, H.O., 1925. Description and theory of the torsion seismometer, *Bull. seism. Soc. Am.*, **15**, 1–72.

Braunmiller, J., Kradolfer, U., Baer, M. & Giardini, D., 2002. Regional moment tensor determination in the European-Mediterranean area—initial results, *Tectonophysics*, **356**, 5–22.

Castellaro, S., Mulargia, F. & Kagan, Y.Y., 2006. Regression problems for magnitudes, *Geophys. J. Int.*, **165**, 913–930.

Castello, B., Olivieri, M. & Selvaggi, G., 2007. Local and duration magnitude determination for the Italian Earthquake Catalog, 1981–2002, *Bull. seism. Soc. Am.*, **97**, 128–139.

Console, R. & Murru, M., 2001. A simple and testable model for earthquake clustering, *J. geophys. Res.*, **106**(B5), 8699–8711.

Console, R., Murru, M. & Alessandrini, B., 1993. Foreshock statistics and their possible relationship to earthquake prediction in the Italian region, *Bull. seism. Soc. Am.*, **83**(4), 1248–1263.

Console, R., Di Luccio, F., Murru, M., Imoto, M. & Stavrakakis, G., 1999. Short term and short range seismicity patterns in different seismic areas of the world, *Nat. Hazards*, **19**(2–3), 107–121.

Console, R., Murru, M. & Lombardi, A.M., 2003. Refining earthquake clustering models, *J. geophys. Res.*, **108**(B10), 2468–2476.

CSTI Working Group, 2005. 'Catalogo strumentale dei terremoti Italiani dal 1981 al 1996, Version 1.1'. Available at: http://gaspy.df.unibo.it/paolo/gndt/Versione1_1/Leggimi.htm, last accessed 1 August 2016.

Dieterich, J.H., 1994. A constitutive law for rate of earthquake production and its application to earthquake clustering, *J. geophys. Res.*, **99**, 2601–2618.

Di Luccio, F., Console, R., Imoto, M. & Murru, M., 1997. Analysis of short time-space seismicity patterns in Italy, *Ann. Geofis.*, **40**(4), 783–798.

Dziewoński, A.M., Chou, T.-A. & Woodhouse, J., 1981. Determination of earthquake source parameters from waveform data for studies of global and regional seismicity, *J. geophys. Res.*, **86**, 2825–2852.

Ekström, G., Nettles, M. & Dziewoński, A.M., 2012. The global CMT project 2004–2010: centroid-moment tensors for 13 017 earthquakes, *Phys. Earth planet. Inter.*, **200–201**, 1–9.

Fuller, W.A., 1987. *Measurement Error Models*, Wiley, 440 pp.

Gasperini, P., 2004. Catalogo dei terremoti CPTI2-Appendice 1, in *Redazione della mappa di pericolosità sismica prevista dall'ordinanza PCM del 20 marzo 2003, n. 3274, Rapporto conclusivo*, Stucchi, M. (Coordinator), Istituto Nazionale di Geofisica e Vulcanologia, Milan, 29 pp. Also available at: http://zonesismiche.mi.ingv.it/documenti/App1.pdf; in Italian.

Gasperini, P., Lolli, B., Vannucci, G. & Boschi, E., 2012. A comparison of moment magnitude estimates for the European-Mediterranean and Italian regions, *Geophys. J. Int.*, **190**, 1733–1745.

Gasperini, P., Lolli, B. & Vannucci, G., 2013. Empirical Calibration of Local Magnitude Data Sets Versus Moment Magnitude in Italy, *Bull. seism. Soc. Am.*, **103**, 2227–2246.

Grandori, G., Guagenti, E. & Perotti, F., 1988. Alarm systems based on a pair of short-term earthquake precursors, *Bull. seism. Soc. Am.*, **78**, 1538–1549.

Grünthal, G., 1998. European macroseismic scale 1998, *Cah. Cent. Eur. Géodyn. Séism.*, **13**, 1–99.

Gutenberg, B. & Richter, C.F., 1944. Frequency of earthquakes in California, *Bull. seism. Soc. Am.*, **34**, 185–188.

Jones, L.M., 1984. Foreshocks (1966–1980) in the San Andreas system, California, *Bull. seism. Soc. Am.*, **74**, 1361–1380.

Jones, L.M., 1985. Foreshocks and time-dependent earthquake hazard assessment in southern California, *Bull. seism. Soc. Am.*, **75**, 1669–1680.

Jones, L.M., 1995. Foreshocks, aftershocks, and earthquake probabilities: accounting for the landers earthquake, *Bull. seism. Soc. Am.*, **84**, 892–899.

Jordan, T.H. *et al.*, 2011. Operational earthquake forecasting: state of knowledge and guidelines for implementation, final report of the international commission on earthquake forecasting for civil protection, *Ann. Geophys.*, **54**(4), 315–391.

Jordan, T.H., Marzocchi, W., Michael, A.J. & Gerstenberger, M.C., 2014. Operational earthquake forecasting can enhance earthquake preparedness, *Seismol. Res. Lett.*, **85**(5), 955–959.

Kagan, Y.Y., 2014. *Earthquakes*, AGU-Wiley, 283 pp.

Kagan, Y.Y. & Jackson, D.D., 1991. Long-term earthquake clustering, *Geophys. J. Int.*, **104**, 117–133.

Kalbfleish, J.G., 1985. *Probability and Statistical Inference, Volume 1: Probability*, Springer-Verlag, 343 pp.

Kisslinger, C., 1993. The stretched exponential function as an alternative model for aftershock decay rate, *J. geophys. Res.*, **98**, 1913–1921.

Lolli, B., Gasperini, P. & Boschi, E., 2011. Time variations of aftershock decay parameters of the 2009 April 6 L'Aquila (central Italy) earthquake: evidence of the emergence of a negative exponential regime superimposed to the power law, *Geophys. J. Int.*, **185**, 764–774.

Marzocchi, W. & Lombardi, A.M., 2008. A double branching model for earthquake occurrence, *J. geophys. Res.*, **113**, B08317, doi:10.1029/2007JB005472.

Marzocchi, W. & Lombardi, A.M., 2009a. Double branching model to forecast the next $M \geq 5.5$ earthquakes in Italy, *Tectonophysics*, **475**, 514–523.

Marzocchi, W. & Lombardi, A.M., 2009b. Real-time forecasting following a damaging earthquake, *Geophys. Res. Lett.*, **36**, L21302, doi:10.1029/2009GL040233.

Mulargia, F. & Geller, R.J., 2003. *Earthquake Science and Seismic Risk Reduction*, Kluwer, 338 pp.

Narteau, C., Shebalin, P., Hainzl, S., Zöller, G. & Holschneider, M., 2003. Emergence of a band-limited power law in the aftershock decay rate of a slider-block model, *Geophys. Res. Lett.*, **30**, 1568, doi:10.1029/2003GL017110.

Ogata, Y., 1988. Statistical models for earthquake occurrences and residual analysis for point processes, *J. Am. Stat. Assoc.*, **83**, 9–27.

Omori, F., 1894. On after-shocks of earthquakes, *J. Coll. Sci. Imp. Univ. Tokyo*, **7**, 111–200.

Parsons, T., Segou, M. & Marzocchi, W., 2015. The global aftershock zone, *Tectonophysics*, **618**, 1–34.

Pondrelli, S., Salimbeni, S., Ekströom, G., Morelli, A., Gasperini, P. & Vannucci, G., 2006. The Italian CMT dataset from 1977 to the present: an extended view of the seismotectonics of this region, *Phys. Earth planet. Inter.*, **159**, 286–303.

Pondrelli, S., Salimbeni, S., Morelli, A., Ekström, G., Postpischl, L., Vannucci, G. & Boschi, E., 2011. European–mediterranean regional centroid moment tensor catalog: solutions for 2005–2008, *Phys. Earth planet. Inter.*, **185**, 74–81.

Postpischl, D., 1985. Catalogo dei terremoti italiani dall'anno 1000 al 1980, *Quad. Ric. Sci.*, **114**(2B), 239 pp.

Savage, M.K. & De Polo, D.M., 1993. Foreshock probabilities in the western Great Basin eastern Sierra Nevada, *Bull. seism. Soc. Am.*, **83**, 1910–1938.

Scognamiglio, L., Tinti, E. & Michelini, A., 2009. Real-time determination of seismic moment tensor for the Italian region, *Bull. seism. Soc. Am.*, **99**, 2223–2242

Sieberg, A., 1931. Erdebeben, in *Handbuch der Geophysik*, Vol. 4, pp. 552–554, ed. Gutenberg, B., Gebrüder Borntraeger (in German).

Sipkin, S.A., 1982. Estimation of earthquake source parameters by the inversion of wave-form data: synthetic waveforms, *Phys. Earth planet. Inter.*, **30**, 242–259.

Sipkin, S.A., 1994. Rapid determination of global moment-tensor solutions, *Geophys. Res. Lett.*, **21**(16), 1667–1670.

Stromeyer, D., Grünthal, G. & Wahlström, R., 2004. Chi-square regression for seismic strength parameter relations, and their uncertainties, with applications to an M_w based earthquake catalog for central, northern and north-western Europe, *J. Seismol.*, **8**(1), 143–153.